CHINESE OPTICS LETTERS

Vol. 21, No. 5 | May 2023

Effect of delay time between pre-pulse and main pulse on single-pass and double-pass amplification of 46.9 nm laser

Dongdi Zhao (赵东迪), Yongpeng Zhao (赵永蓬)*, Huaiyu Cui (崔怀愈), Bo An (安 博), Lei Li (李 镭), and Yunsong Bai (白云松)

National Key Laboratory of Science and Technology on Tunable Laser, Harbin Institute of Technology, Harbin 150080, China

*Corresponding author: zhaoyp3@hit.edu.cn

Received November 29, 2022 | Accepted March 7, 2023 | Posted Online April 20, 2023

In this paper, the influence of the delay time between the pre-pulse and the main pulse on the double-pass amplified 46.9 nm laser was studied for the first time, to the best of our knowledge, by using a high-precision polished SiC slice as a rear mirror. The temporal and spatial characteristics of the output laser were measured separately to investigate the effect of the delay time on the laser characteristics. The energy of the double-pass amplified laser was between 510 μJ and 890 μJ. In addition, a theoretical model of double-pass amplification was established to analyze the effect of the delay time on the double-pass amplified 46.9 nm laser.

Keywords: double-pass amplification; delay time; 46.9 nm laser; capillary discharge.

DOI: 10.3788/COL202321.053401

1. Introduction

In order to generate the 46.9 nm laser pumped by the fast capillary discharge, it is necessary to use a pre-pulse current with an amplitude of tens of amperes to pre-ionize the Ar gas in the capillary into an initial plasma. After a specific delay time, the initial plasma is pinched by the main pulse current to generate the plasma column with a high electron density and a high electron temperature and an output of Ne-like Ar 46.9 nm laser. In 1994, Rocca *et al.* achieved the first 46.9 nm laser output by a fast capillary discharge device[1]. The delay time between the pre-pulse and the main pulse in this experiment was about 2 μs. After that, the researchers carried out a detailed study on the effect of the pre-pulse current on the 46.9 nm laser. In 2007, Tan *et al.* studied the effect of delay time between the pre-pulse and the main pulse on the 46.9 nm laser[2]. It was found that the laser intensity increased significantly in the range of 2 μs to 4 μs, the laser intensity was less affected by the delay time in the range of 4 μs to 30 μs, and the laser intensity decreased rapidly with the increase of the delay time when the delay time exceeded 30 μs.

In 2012, our group carried out a corresponding study on the influence of the delay time on the output laser intensity in the range of 2–130 μs[3]. It was found that the laser intensity reached the maximum when the delay time was 12 μs, and the laser intensity changed slowly when the delay time was longer than 40 μs. The above results show the effect of the delay time on the temporal characteristics of the 46.9 nm laser. However, there is little research on the relationship between the spatial characteristics of the 46.9 nm laser and the delay time, and all the above experiments are based on the single-pass amplified laser experiments without a cavity. Rocca *et al.* carried out the first double-pass amplified 46.9 nm laser experiment in the world with an Ir mirror in 1996[4]. However, the Ir mirror would be damaged by the plasma column after 1–3 discharge shots. Therefore, their team did not provide the experimental results of the temporal and spatial characteristics of the double-pass amplified 46.9 nm laser. In 2021, our group obtained the double-pass amplified 46.9 nm laser with a SiC mirror[5], but we only provided the experimental results corresponding to one kind of spatial distribution. According to our theoretical results, the spatial distribution will affect the double-pass amplification of the 46.9 nm laser. Therefore, it is necessary to change the laser spatial distribution in the double-pass amplification experiments. In previous experiments, we found that the delay time between the pre-pulse and the main pulse can change the spatial distribution of the laser.

In this paper, to the best of our knowledge, the relationship between the double-pass amplified 46.9 nm laser and the delay time was studied for the first time. In order to study the effect of the delay time on the spatial characteristics of the 46.9 nm laser in detail, we used a theoretical model to simulate the spatial distribution of the single-pass and double-pass amplified 46.9 nm lasers. In previous reports, many groups have used the ray-tracing code to simulate the spatial distribution of the X-ray laser[6–9]. However, to the best of our knowledge, there is no report on the theoretical model of the double-pass amplified 46.9 nm laser.

In the experiment, the characteristics of the single-pass and double-pass amplified 46.9 nm lasers with different delay times were measured. In theory, a theoretical model was built to study the laser spatial distributions of the single-pass and double-pass amplified 46.9 nm laser. This theoretical model constructed by the ray-tracing code was used to simulate the spatial distributions of the 46.9 nm laser with different electron density distributions and gain coefficient distributions. The experimental results about the double-pass amplified 46.9 nm laser will help to improve the laser performance and to expand the application range of the 46.9 nm laser.

2. Experimental Setup

The capillary discharge device used in this study has been introduced in the previous paper[10]. The capillary used in this experiment was an Al_2O_3 capillary with a length of 35 cm and an inner diameter of 3.2 mm. 20 Pa of Ar was filled into it and ionized into an initial plasma column by a 20 A pre-pulse current. After a delay time of 10–75 μs, the main pulse current was generated by the Marx generator and by a Blumlein transmission line with a current amplitude of 13 kA. The main pulse current flowed through the initial plasma and encompassed the initial plasma into the suitable state for laser generation by the Z-pinch effect. First, we carried out the single-pass amplification experiment without the resonator. After measuring the single-pass amplified laser characteristics, a SiC slice was placed 2.5 cm away from the end of the capillary to provide a feedback laser, which could re-enter the plasma column to generate the double-pass amplified laser. In this experiment, an X-ray diode (XRD) with a gold-coated cathode and metal mesh anode was used to measure the laser pulse. An X-ray CCD (charged-coupler device, Andor DO934P-BN) with a resolution of 1024 × 1024 was used to measure the laser spot to study the laser spatial characteristics.

3. Experimental Results and Discussions

Firstly, the spatial characteristics of the single-pass amplified laser corresponding to different delay times between the pre-pulse and the main pulse were measured. Here, we selected three typical laser spots, which correspond to the delay times of 10 μs, 60 μs, and 75 μs, as shown in Fig. 1. When the delay time is 10 μs, the laser spot shows a single annular-shaped distribution, and the peak-to-peak divergence is 2.6 mrad. The single annular-shaped distribution is formed by the refraction of the X-rays in the plasma column. The refraction effect is related to the electron density gradient in the radial direction. When the delay time is 60 μs, the laser spot shows a double annular-shaped distribution, and the peak-to-peak divergence of the outer annulus is 3.1 mrad. When the delay time is 75 μs, the laser spot also shows a double annular-shaped distribution, and the peak-to-peak divergence of the outer annulus is 2.6 mrad. The possible formation reason for the double annular-shaped distribution is that some X-rays in the small density gradient region will propagate in the plasma column at a small angle and be concentrated near the axis, which has been introduced in the previous paper[9].

After measuring the laser spatial distributions of the single-pass amplified laser and selecting three typical laser spots, the laser pulses corresponding to the three delay times were measured by XRD, as shown in Fig. 2. When the delay time is 10 μs, the laser signal amplitude is 6.8 V, the laser energy is about 290 μJ, and the laser pulse width is 1.2 ns. When the delay time is 60 μs, the laser signal amplitude is 5.4 V, the laser energy is about 240 μJ, and the laser pulse width is 1.1 ns. When the delay time is 75 μs, the laser signal amplitude is 5.4 V, the laser energy is about 260 μJ, and the laser pulse width is 1.2 ns. In Ref. [3], it was found that the laser intensity reached the highest at about 12 μs and

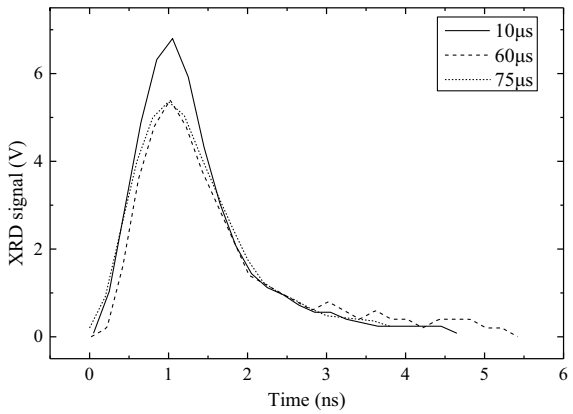

Fig. 2. The laser pulse signals corresponding to different delay times.

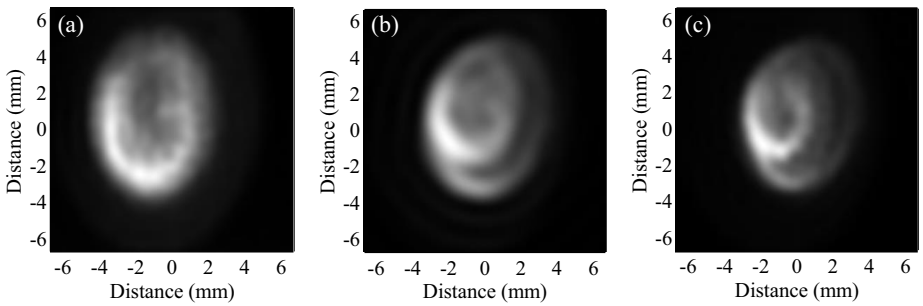

Fig. 1. Laser spatial distributions corresponding to delay times between pre-pulse and main pulse of (a) 10 μs, (b) 60 μs, and (c) 75 μs.

changed little after 40 μs. The results in this paper are consistent with Ref. [3]. Therefore, it can be seen that the delay time can influence the laser energy and the spatial distribution of the single-pass amplified 46.9 nm laser.

Next, a high-precision polished SiC mirror was placed at the end of the capillary to realize the double-pass amplification experiment. Figure 3 shows the double-pass amplified laser spots. Comparing the single-pass amplified laser spots in Fig. 1 with the double-pass amplified laser spots in Fig. 3, it can be found that the spatial distributions are quite different. When the delay time is 10 μs, it changes from the single annular-shaped distribution to the double annular-shaped distribution. The peak-to-peak divergence of the outer annulus of the double-pass amplified laser is about 3.2 mrad, 0.6 mrad more than that of the single-pass amplified laser. When the delay time is 60 μs, for the single-pass amplified laser, the peak amplitudes of the inner annulus and the outer annulus are nearly equal. However, for the double-pass amplified laser, the peak amplitude of the outer annulus is nearly 1.6 times as large as that of the inner annulus, and the peak-to-peak divergence of the outer annulus is about 3.2 mrad, which is nearly equal to that of the single-pass amplified laser. When the delay time is 75 μs, for the single-pass amplified laser, the peak amplitude of the inner annulus is nearly twice as large as that of the outer annulus. However, for the double-pass amplified laser, the peak amplitude of the outer annulus increases more than that of the inner annulus, and the peak-to-peak divergence of the outer annulus is about 2.6 mrad, which is nearly equal to that of the single-pass amplified laser.

Finally, the temporal characteristic of the double-pass amplified 46.9 nm laser was measured by XRD. As shown in Fig. 4, the delay time affected the amplitude and width (full-width at half-maximum) of the double-pass amplified laser pulse. When the delay time is 10 μs, the laser signal amplitude is 10.0 V, the laser energy is about 560 μJ, and the laser pulse width is 1.8 ns. When the delay time is 60 μs, the laser signal amplitude is 13.0 V, the laser energy is about 890 μJ, and the laser pulse width is 2.0 ns. When the delay time is 75 μs, the laser signal amplitude is 8.0 V, the laser energy is about 510 μJ, and the laser pulse width is 1.7 ns. The reason why only one peak can be seen in Fig. 4 is the partial overlap and addition of the first-pass and the second-pass laser pulses.

Table 1 shows the double-pass amplification compared with the single-pass amplification corresponding to the different delay times. As shown in Table 1, the double-pass amplification of 60 μs has the largest laser signal amplitude, the largest magnification, and the widest laser pulse width. Therefore, the feedback laser is amplified most obviously at 60 μs among the three delay times rather than at 10 μs. This may be caused by the fact that more X-rays are concentrated near the axis when the delay time is 60 μs. The X-ray concentrated near the axis has a small divergence angle, which allows more X-rays to enter the plasma column after the reflection from the SiC mirror. This means that the intensity of the feedback laser when the delay time is 60 μs is higher than that of 10 μs.

It can be found that the double-pass amplification effects are different with different delay times. We attribute this to the difference in the electron density distributions and gain coefficient distributions corresponding to the different delay times. In order

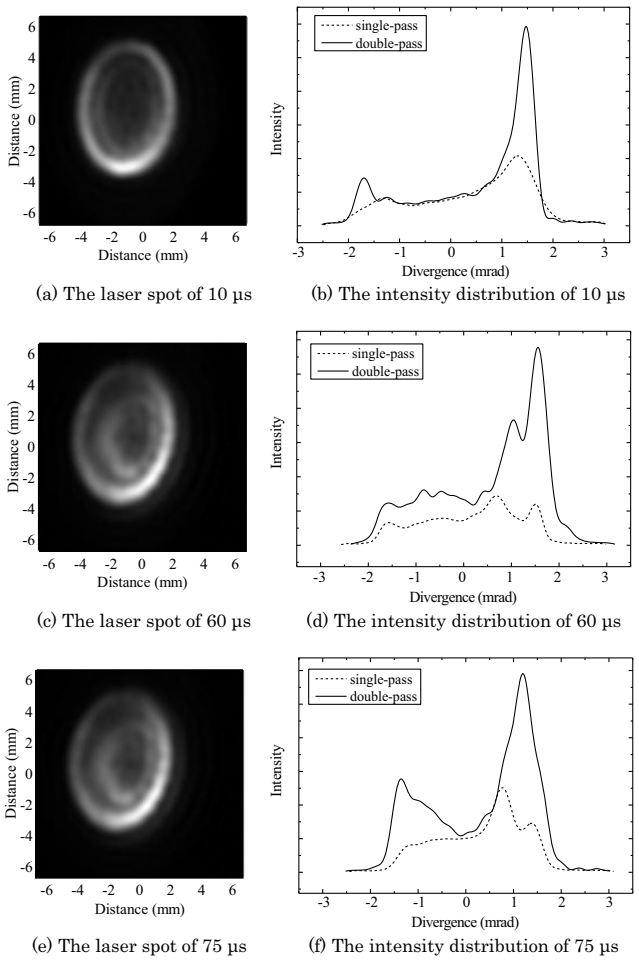

Fig. 3. The double-pass amplified laser spots and their intensity distributions.

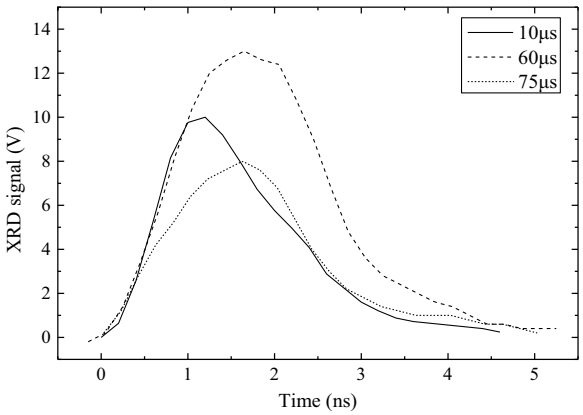

Fig. 4. The double-pass amplified laser pulse signals corresponding to different delay times.

Table 1. The Double-pass Amplification Compared with the Single-pass Amplification Corresponding to Different Delay Times.

Delay Time (μs)	Single-pass Amplified Laser Energy (μJ)	Double-pass Amplified Laser Energy (μJ)	Magnification in the Laser Energy	Laser Pulse Width of the Single-pass Amplification (ns)	Laser Pulse Width of the Double-pass Amplification (ns)	Increase in the Laser Pulse Width (ns)
10	290	560	1.93	1.2	1.8	0.6
60	240	890	3.71	1.1	2.0	0.9
75	260	510	1.96	1.2	1.7	0.5

to prove this analysis, a theoretical model based on the ray-tracing code was used to simulate the spatial distributions of single-pass and double-pass amplified 46.9 nm lasers. The theoretical model of the single-pass amplified 46.9 nm laser is established according to the theories introduced in Refs. [6,7]. Based on this theoretical model, the feedback laser reflected by the mirror is considered in the theoretical model during the calculation of the double-pass amplified laser spot. The intensity of the feedback laser is $I_f = R \cdot I_s$, where R is the reflectivity of the SiC mirror, and I_s is the intensity of the single-pass amplified laser. The position where the feedback laser re-enters into the end of the plasma column is regarded as the initial position of the second-pass amplified laser. Based on the intensity and the initial position of the feedback laser, the intensity of the second-pass amplified laser can be calculated by the ray-tracing code. With the theoretical model, the laser spatial distribution can be calculated by setting the electron density distribution and gain coefficient distribution.

Many different types of electron density distributions and gain coefficient distributions have been tried in order to make the simulation spot close to the experimental spot. During the calculation, we found that some different types of curves can obtain similar results to the experimental single-pass amplified laser spot or double-pass amplified laser spot. However, it was hard to find curves that fit both the laser spots. Figure 5 shows a set of curves that are suitable for the experimental single-pass amplified laser spot and double-pass amplified laser spot. We considered that these electron density distributions and gain coefficient distributions may be close to the actual distributions.

Figures 6–8 show the single-pass amplified and double-pass amplified laser spatial distributions and the intensity distributions in the vertical direction calculated by using the theoretical model. In order to compare with experimental results, the intensity distributions corresponding to the laser spot in Figs. 1 and 3 are also shown in Figs. 6–8. As shown in Figs. 6–8, the simulation spatial distributions are close to the experimental spatial distributions. The divergences of the simulation laser spots are nearly equal to that of the experimental laser spots. The simulation ratios between the inner annulus' peak amplitudes and the outer annulus' peak amplitudes are also nearly equal to the experimental ratios. Therefore, we consider that the variation of the plasma column state at the time of maximum laser intensity, including the electron density fraction and gain coefficient distribution, results in the variation of the laser energy and spatial distribution.

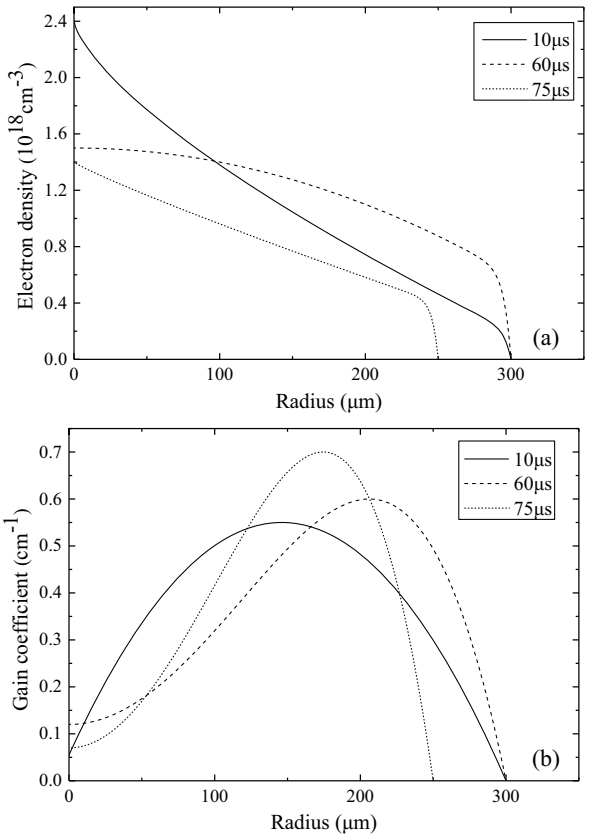

Fig. 5. The radial distributions of (a) the electron density and (b) the gain coefficient corresponding to different delay times.

Based on the theoretical simulation results in Figs. 5–8, we can explain that the best delay time for double-pass amplification is 60 μs rather than 10 μs. The refraction effect is one of the main factors affecting the 46.9 nm laser intensity, especially in the process of double-pass amplification. The refraction effect may cause the feedback laser to emit from the edge of the plasma column very early. Therefore, the second-pass amplified laser may only have a small gain length product. As shown in Fig. 5, the laser output from the plasma column at 60 μs has a smaller electron density gradient compared to that at 10 μs.

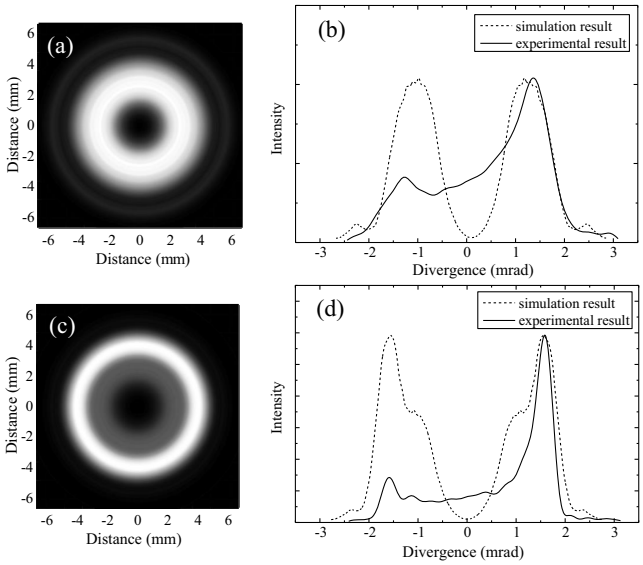

Fig. 6. The simulation spot and the intensity distribution in the vertical direction of (a), (b) the single-pass amplified laser and (c), (d) the double-pass amplified laser at 10 μs.

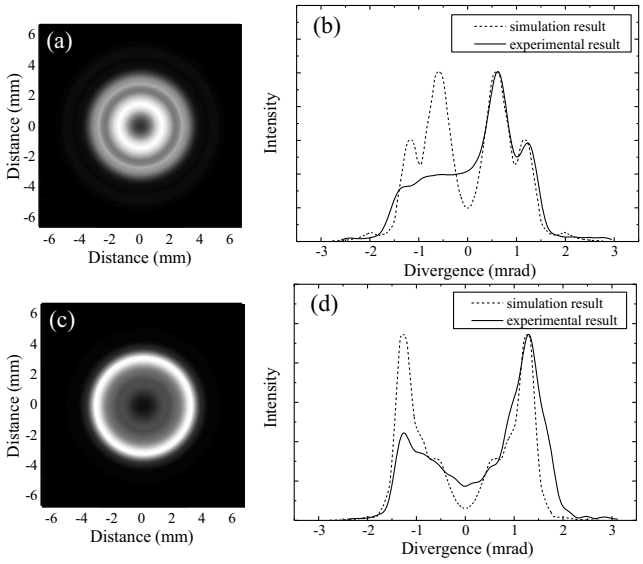

Fig. 8. The simulation spot and the intensity distribution in the vertical direction of (a), (b) the single-pass amplified laser and (c), (d) the double-pass amplified laser at 75 μs.

The feedback laser is less affected by the refraction effect when propagating in the plasma column. This results in a larger gain length product for the second-pass amplified laser. Compared to 10 μs, the double-pass amplification of 60 μs has a larger feedback laser intensity and a larger gain length product for the second-pass amplified laser. Therefore, 60 μs is more suitable than 10 μs for double-pass amplification. We attribute the variation of the plasma column state with the delay time to the radial inhomogeneity of the initial plasma column introduced in Ref. [11]. In Ref. [11], it is found that the initial plasma generated by the pre-pulse is radially inhomogeneous and changes with time. Therefore, when the main pulse flows through the initial plasma at different delay times, the state of the plasma column generated by the main pulse will be different. As a result, the laser energy, spatial distribution, and double-pass amplification effect corresponding to different delay times are different.

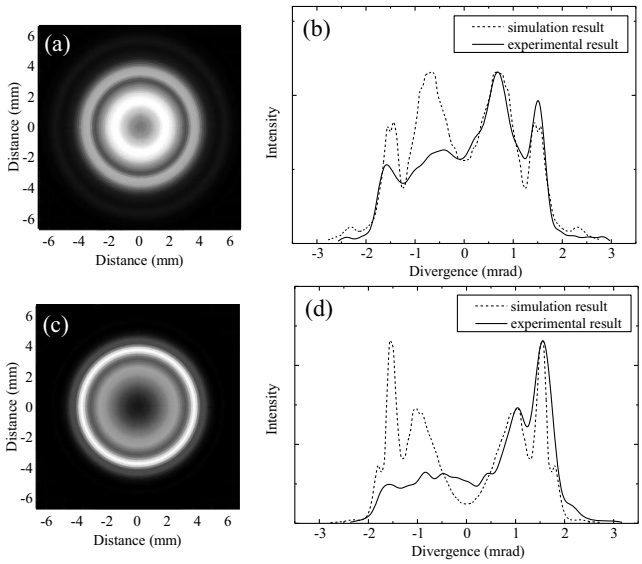

Fig. 7. The simulation spot and the intensity distribution in the vertical direction of (a), (b) the single-pass amplified laser and (c), (d) the double-pass amplified laser at 60 μs.

4. Conclusion

In this paper, a series of single-pass and double-pass amplified 46.9 nm laser experiments are carried out by changing the delay time between the pre-pulse and the main pulse. To the best of our knowledge, this is the first regular experiment with the double-pass amplified 46.9 nm laser in the world. For the single-pass amplification, in terms of the temporal characteristics, the laser energy at 10 μs is the largest, the laser energy at 60 μs is larger than that at 75 μs, and their pulse widths are nearly equal. In terms of the spatial characteristics, the laser spot at 10 μs shows a single annular-shaped distribution, the laser spots at 60 μs and 75 μs show double annular-shaped distributions, and the peak-to-peak divergence decreases gradually with the increase of the delay time. For the double-pass amplification, in terms of temporal characteristics, the double-pass amplified laser at 60 μs has the highest laser signal energy and the widest laser signal width. Compared with the single-pass amplified laser signal, the energy enhancement of the double-pass amplified laser pulse was about 3.6×, and the full-width at half-maximum of the double-pass amplified pulse broadened by about 0.9 ns. The double-pass amplified laser energy magnification and increased width at 10 μs are 1.9× and 0.6 ns, respectively. The double-pass amplified laser energy magnification and increased width at 75 μs are

1.9× and 0.5 ns, respectively. In terms of the spatial characteristics, the laser spots at all the three delay times show a double annular-shaped distribution. The intensity of the outer annulus is larger than that of the inner annulus, and the peak-to-peak divergence of the outer annulus decreases gradually with the increase of the delay time.

In theory, we obtain the simulation laser spatial distributions, which are similar to the experimental results, by using the theoretical model. By analyzing the results, we find that the plasma column with a small electron density gradient is more suitable for double-pass amplification. In addition, we consider that the variation of the plasma column state at the time of maximum laser intensity will affect the laser characteristics of single-pass amplification and double-pass amplification. This variation may be related to the initial plasma state. In conclusion, changing the delay time can change the single-pass laser characteristics and the double-pass amplification effect. This can provide larger energy and wider pulse width of the 46.9 nm laser and help broaden the application range of the 46.9 nm laser. In future work, we will continue to explore the influence of the initial plasma state on laser characteristics.

Acknowledgement

This work was supported by the National Natural Science Foundation of China (Nos. 61875045 and 62005066).

References

1. J. J. Rocca, V. Shlyaptsev, F. G. Tomasel, O. D. Cortázar, D. Hartshorn, and J. L. A. Chilla, "Demonstration of a discharge pumped table-top soft-X-ray laser," Phys. Rev. Lett. **73**, 2192 (1994).
2. C. A. Tan and K. H. Kwek, "Influence of current pre-pulse on capillary-discharge extreme-ultraviolet laser," Phys. Rev. A **75**, 043808 (2007).
3. S. Jiang, Y.-P. Zhao, Y. Xie, M. Xu, H.-Y. Cui, H. Wu, Y. Liu, Q. Xu, and Q. Wang, "Observation of capillary discharge Ne-like Ar 46.9 nm laser with pre-pulse and main-pulse delay time in the domain of 2–130 μs," Appl. Phys. B **109**, 1 (2012).
4. J. J. Rocca, D. P. Clark, J. L. A. Chilla, and V. N. Shlyapstev, "Energy extraction and achievement of the saturation limit in a discharge-pumped table-top soft X-ray amplifier," Phys. Rev. Lett. **77**, 1476 (1996).
5. Y. Zhao, D. Zhao, B. An, L. Li, Y. Bai, and H. Cui, "Demonstration of double-pass amplification of gain saturated 46.9 nm laser," Opt. Commun. **506**, 127571 (2021).
6. R. A. London, "Beam optics of exploding foil plasma X-ray lasers," Phys. Fluids **31**, 184 (1988).
7. J. L. A. Chilla and J. J. Rocca, "Beam optics of gain-guided soft-X-ray lasers in cylindrical plasmas," J. Opt. Soc. Am. B **13**, 2841 (1996).
8. A. Ritucci, G. Tomassetti, A. Reale, F. Flora, and L. Mezi, "Coherence properties of a quasi-Gaussian submilliradiant divergence soft-X-ray laser pumped by capillary discharges," Phys. Rev. A **70**, 023818 (2004).
9. Y. P. Zhao, D. D. Zhao, Q. Yu, M. U. Khan, H. Q. Lu, J. J. Li, and H. Y. Cui, "Influence of He mixture on the pulse amplitude and spatial distribution of an Ne-like Ar 46.9 nm laser under gain saturation," J. Opt. Soc. Am. B **37**, 2271 (2020).
10. Y. P. Zhao, Y. L. Cheng, B. H. Luan, Y. C. Wu, and Q. Wang, "Effects of capillary discharge current on the time of lasing onset of soft X-ray laser at low pressure," J. Phys. D **39**, 342 (2006).
11. S. Elissev, M. Timshina, A. Samokhvalov, Y. P. Zhao, and V. Burtsev, "Plasma dynamics at the preionization stage in discharge-based EUV lasers," J. Phys. D **54**, 095201 (2021).